Hindawi
Geofluids
Volume 2022, Article ID 1874331, 18 pages
https://doi.org/10.1155/2022/1874331

Research Article

An Innovative Balanced-Yielding Support Method for Tunnel in Deep Inclined Strata

Wei Yongke,[1] Guo Hongyan,[2,3] Hu Juyi,[3] Liu Jiaqing,[1] and Liu Limin[4]

[1]*Guangxi Xinfazhan Communications Group Co., Ltd., Nanning, 530029 Guangxi, China*
[2]*College of Civil Engineering, Chongqing University, Chongqing 400044, China*
[3]*China Merchants Chongqing Communications Technology Research & Design Institute Co., Ltd., Chongqing 400067, China*
[4]*College of Energy and Mining Engineering, Shandong University of Science and Technology, Qingdao, Shandong 266590, China*

Correspondence should be addressed to Guo Hongyan; 717692502@qq.com

Received 8 July 2022; Accepted 3 August 2022; Published 16 August 2022

Academic Editor: Zhengzheng Xie

Aiming at the problem that the uneven deformation of the tunnel surrounding rock in the deep inclined rock strata caused local instability, an innovative balanced-yielding support technology was proposed with the engineering background of the Shangping tunnel in Huafeng Mine. Based on the mechanism analysis of this technology, the specific implementing steps were proposed. It mainly included in situ stress analysis, the stress distribution of the tunnel surrounding rock with different sections, the design of the parameter of bolt-cable and yielding structure, and supporting effect evaluation. The results showed that (1) the stress concentration appeared at the top corners of the lower side and the bottom corner of the upper side of the rectangular and semicircular arched tunnel. (2) Compared with rectangle and vertical-wall semicircular arch tunnels, the trapezoidal tunnel could relieve the shearing effect of the inclined rock strata. (3) The length, prestress, spacing-row distance of the bolt, and the parameter of the yielding structure were all optimally designed to form the balanced-yielding support system. (4) In engineering application, the maximum deformations of the roof, right side and left side, were less than 80 mm. Compared with the original support system, the shallow separation of the trapezoidal tunnel supported by the balanced-yielding support system had been reduced by 147%.

1. Introduction

The underground rock mass is in a state of stress balance before excavation. Manual excavation removes the constraint force in one direction of the rock mass, resulting in an unbalanced state. So, the rock mass will move to the excavated free space to reach a new stress balance state. In order to maintain the stability of the underground rock mass, a certain external force needs to be applied to make up for the original restraining stress. The methods of controlling the stability of the surrounding rock mainly include active support and passive support [1–6]. Passive support only uses the bearing capacity of the support structure itself to resist the stress of the surrounding rock, mainly including shed-type supports, single pillar, U-shaped steel support, and concrete-filled steel tube support. Active support is to reinforce the shallow surrounding rock through the support structure to improve the self-carrying capacity of the rock mass to resist the stress released by the deep rock mass. Active support mainly includes bolts, cables, anchor cables, grouting, and shotcreting.

As the depth of underground engineering gradually increases, ground stress gradually increases. General passive support is difficult to meet the requirements of the controlling deep surrounding rock. Active support was widely used in deep tunnel with its concept of actively reinforcing the surrounding rocks. Among them, bolt and cable supports were the most widely used. In addition, the combined support of bolts and cables can connect the rock masses of different depths, realizing the suspension of shallow bearing arches on deep rock masses [7, 8]. It plays the role of combining the self-loading of the shallow surrounding rock with

Stratum system	Rock	Histogram	Order	Thickness /mm	Strata characteristics	
					Strata characteristics	Compressive strength/MPa
Carbonife–rous taiyuan formation	Siltstone		1	6.0	Grey black, more bedding	46.1
	Medium siltstone		2	2.4	Gray white, thick layered	55.45
	Siltstone		3	1.8	Gray black, more bedding	21.78
	6th coal		4	1.1		18–25.5
	Siltstone		5	1.6	Gray-yellow, more bedding	48.6
	Medium siltstone		6	2.0	Gray white, thick layered	69.5
	Fine siltstone		7	8.5	Gray-black, thick layered	71.2

Figure 1: Partial stratigraphic section of Huafeng Mine.

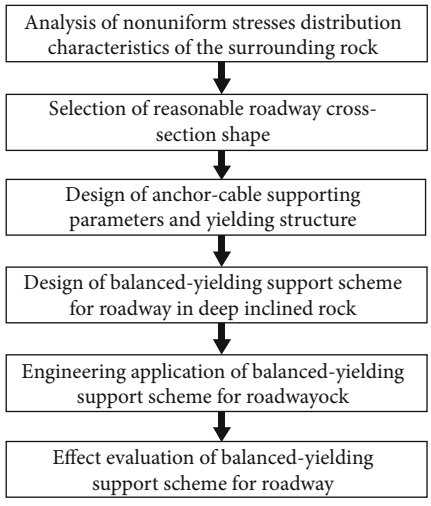

Figure 2: The specific implementing steps of the balanced-yielding support technology.

the deep surrounding rock, and is widely used in deep coal mine tunnels, deep metal mine tunnels, high stress tunnels, etc. [9–12].

For special deep surrounding rock tunnels including dynamic pressurized tunnels, soft rock tunnels, asymmetric surrounding rock tunnels, and inclined rock tunnels, different bolt-cable support schemes are required. Among them, the surrounding rock controlling of the tunnel in deep inclined rock strata has always been a big problem [13–16]. There are two main reasons. On the one hand, the in situ stress of deep rock mass is relatively high. On the other hand, the inclined rock strata make the stress of the tunnel surrounding rock uneven, resulting in local stress concentration [17–20].

Many scholars had investigated the support method for deep inclined rock tunnel. Liang et al. [21] proposed the two-dimensional hydraulic-mechanical calculation model and the key-strata stability analysis model to analyze the theoretical range of failure and the stability of inclined floor strata after mining. Sun et al. [22] investigated the inclination effect of mine strata on the stability of loess land slope under the condition of underground mining. Wang et al. [23] proposed DFH control strategies of the tunnel driven in deep inclined strata. Ye et al. [24] analyzed the fracture evolution characteristics of overlying strata above working face with large inclination angle and mining depth. Sun et al. [25] present an experimental study on the floor heave of tunnel excavated in deep ten degree inclined strata.

Although the above research had played a role in the control of the surrounding rock of the inclined rock strata, the current research and application were both limited. There was no unified design concept. It failed to balance support costs and effects. On the one hand, the supporting parameters were too large, resulting in waste of supporting materials. On the other hand, the supporting parameters were too small, resulting in poor control effect. Due to the local stress concentration of the tunnel surrounding rock in inclined rock strata, the force of local bolts increases too fast and breaks, so the ordinary strong anchor theory is difficult to give full play to its effective role. It is necessary to

Table 1: The measurement results of the in situ stress.

Monitoring points	Buried depth (m)	Vertical stress (MPa)	Maximum horizontal principal stress (MPa)	Minimum horizontal principal stress (MPa)	Direction of maximum horizontal principal stress
1	1220	30.50	42.19	22.80	N3°E
2	1130	28.25	33.15	19.10	N31.5°E
3	1040	26.00	31.35	16.20	N23.5°W

Table 2: Mechanical parameters of the 6th coal roof and floor strata (average).

Lithology	Elastic modulus (GPa)	Poisson's ratio	Cohesion (MPa)	Internal friction angle (°)	Uniaxial tensile strength (MPa)	Uniaxial compression strength (MPa)	Bulk density ($kg \cdot m^{-3}$)
Sandstone	26	0.13	17	22	6.1	70	2600
Mudstone	6	0.35	4.6	16	2.3	26	2500
Coal	5	0.37	4.2	15	2.1	24	1300
Medium sandstone	21	0.18	12	18	5.4	38	2600
Siltstone	40	0.25	7.5	32	9.0	47	2550

adopt the yield-antibalance combination concept. The rod is protected by yielding structure to give full play to the role of the high-strength bolt. Then, the asymmetrical surrounding rock stress is balanced by the asymmetrical bolt-cable parameters to achieve the overall balance of the tunnel surrounding rock. The buried depth of the Shangping tunnel of Huafeng Mine in Tai'an, China, is more than 1000 m. The inclination angle of the rock strata is greater than 30°. It belongs to a typical deep inclined rock tunnel. The original support scheme was high-strength bolts with the type of $\Phi 25 \times 2500$ mm and the density of 700×700 mm to control the surrounding rock of the tunnel. Although the strength of the supporting structure was already great, the local surrounding rock deformation was still great, especially part of the bolt had broken.

Taking the Shangping tunnel of Huafeng Mine as the engineering background, the paper innovatively proposed the balanced-yielding support technology for tunnel in the deep inclined rock. Then, the implementation steps were described in detail. This technology reinforced the tunnel surrounding rock by the yielding support structure to eliminate the local stress concentration, achieving that the deformation of the local surrounding rock was basically equal. The technology could achieve the overall balance of the deformation and stress of the tunnel surrounding rock through the asymmetrical yielding support structure.

2. Background

Huafeng Mine is located in Tai'an, Shandong, China. The inclination angle of the 6th coal is 31° to 33°. Figure 1 shows the characteristics of the roof-floor rocks of the 6th coal seam. The elevation of the Shangping tunnel is -922 m. Above and below it are the mined 1610 working face and the unmined 1611 working face, respectively. The strike length of the Shangping tunnel is 400 m. Its average buried depth is 1020 m. The characteristics of large buried depth, large inclination angle, and high ground stress determine the difficulty of surrounding rock control. The original high-strength bolt-net support scheme with the high-strength bolt with the type of $\Phi 25 \times 2500$ mm and the density of 700×700 mm, one cable with the length of 4500 mm in the middle of the roof and the metal net and steel strip laid on the surface was used to control the surrounding rock of the Shangping tunnel. However, the local surrounding rock had a large deformation, so it cannot meet the requirements of normal use. And the bolts in the top corners of the lower side and the bottom corner of the upper side of the tunnel were broken. So, only the high-strength support concept cannot effectively control the stability of the surrounding rock of the Shangping tunnel. Therefore, it is urgent to find a new support concept. Based on the yield-antibalance combination concept, this paper attempted to use prestressed yield bolts to control the surrounding rock in Shangping tunnel.

3. Balanced-Yielding Support Technology for Tunnel in the Deep Inclined Rock

3.1. Proposal. In the deep inclined rock, the component force of the rock layer in the sloping direction causes the nonuniform stresses of the tunnel surrounding rock. The stress concentration occurs in the surrounding rock locally, resulting in uneven damage to the surrounding rock. In order to alleviate the effect of the gravity component of the overlying inclined rock strata, a reasonable cross-sectional shape of the tunnel should be selected first. Then, the nonuniform supporting structure minimizes the stress concentration. That is, the interaction between the supporting structure and the surrounding rock makes the system reach a certain relative balance.

The yielding structure plays a first role in the stress concentration area of the surrounding rock, relieving local excessive stress to reduce the stress concentration, which can promote the overall force of the surrounding rock to be more uniform. So, the yielding support structure can promote the balance of stress and displacement of the

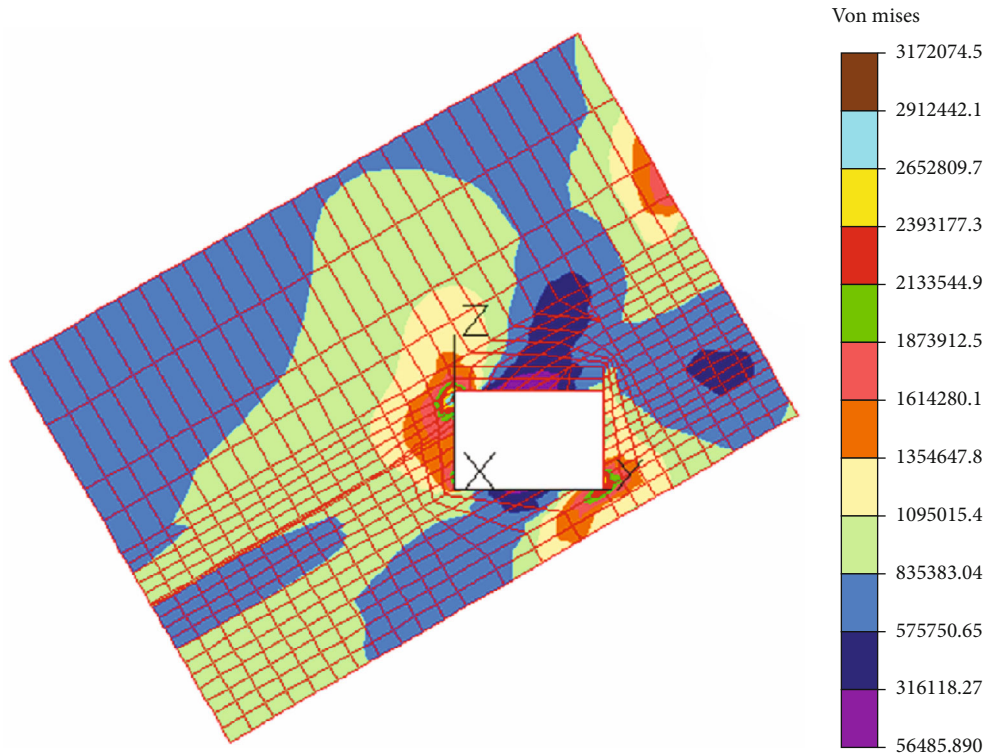

(a) Shear stress distribution

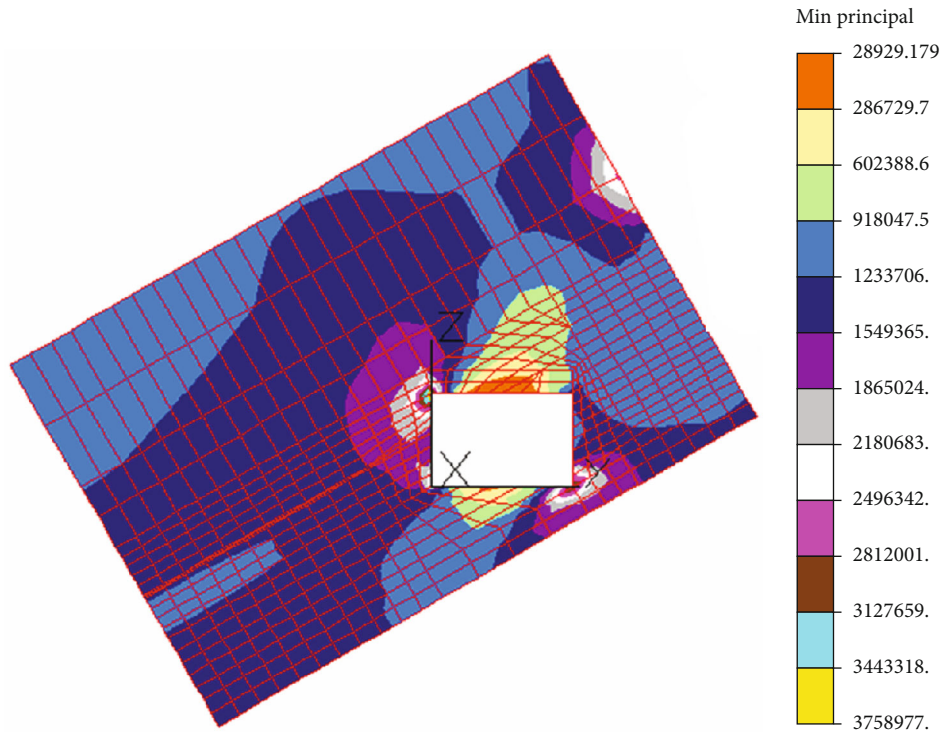

(b) Minimum principal stress distribution

Figure 3: Stress distribution of the surrounding rock of rectangular tunnel.

surrounding rock. The balanced-yielding support technology mainly controls the uneven deformation of the tunnel from the angle of stress and displacement balance through the yielding structure and the asymmetrical anchor cable. The stress balance is achieved by controlling the tensile stress of the asymmetric surrounding rock within a basically symmetrical range by forming a common bearing body between the supporting structure and the surrounding rock.

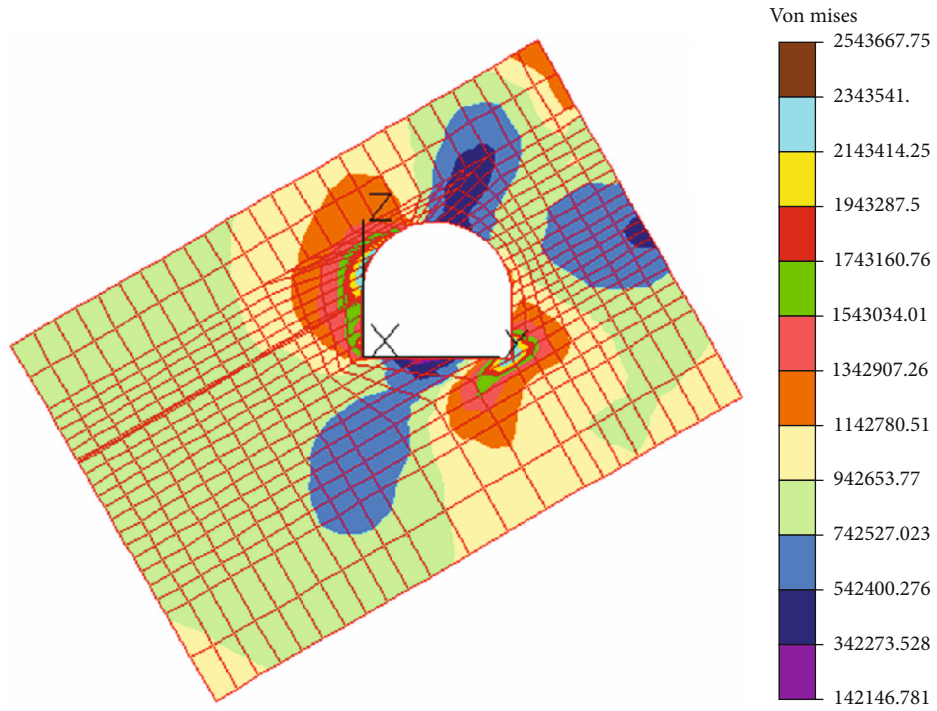

(a) Shear stress distribution

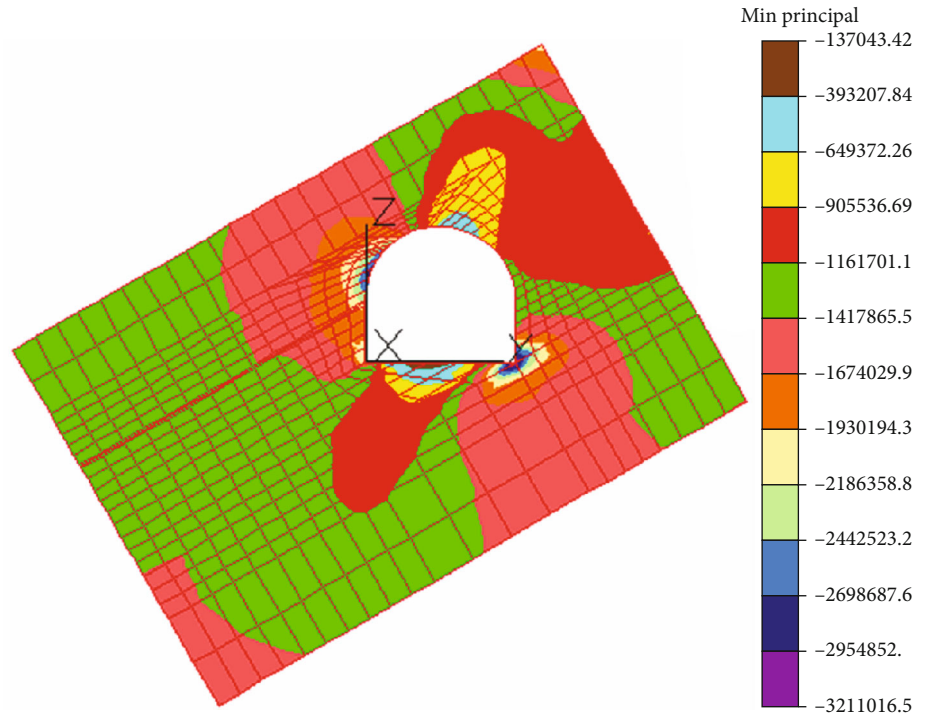

(b) Minimum principal stress distribution

Figure 4: Stress distribution of the surrounding rock of vertical-wall semicircular arch tunnel.

The displacement balance is achieved by controlling the surface displacement of the tunnel in a basically symmetrical range by forming a common bearing body between the supporting structure and the surrounding rock.

The balanced-yielding support technology is applicable to the reinforcement of mine roadways, tunnels, and other underground chambers. In the underground tunnel support system, the surrounding rock is controlled by applying prestress and installing yielding structures to the bolts (cables). The yielding structure can be deformed before the bolt-rod is stressed to the yield strength, so as to achieve controlled yielding. The supporting structure can provide constant

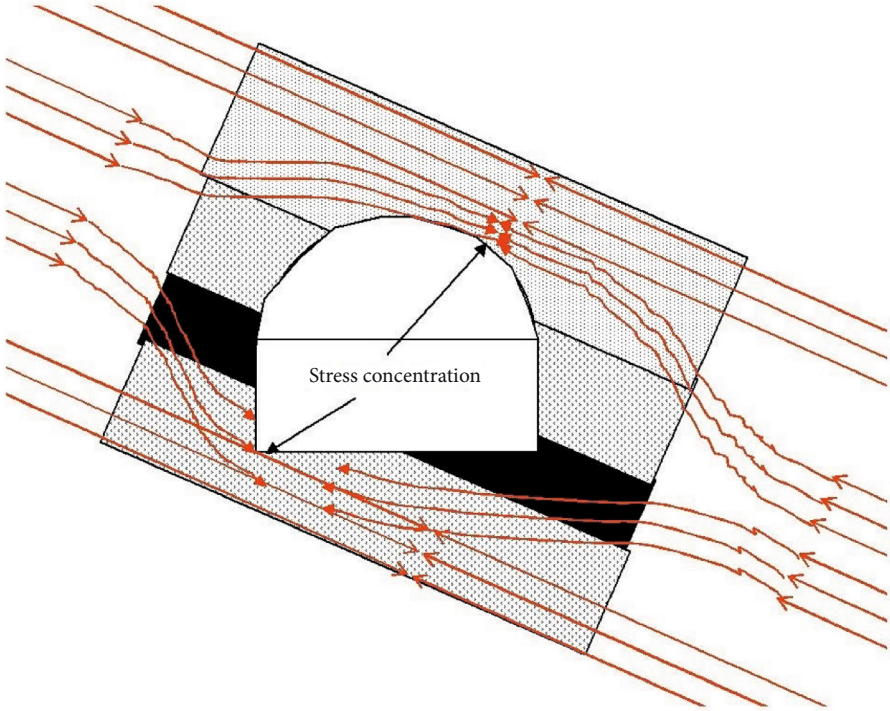

Figure 5: The component force effect of the rock layer's own weight stress in the inclined direction.

supporting resistance for a long time and maintain the long-term stability of the surrounding rock. The layout parameters of prestressed anchor cables should be based on the stress of the tunnel surrounding rock in order to achieve differential active control.

3.2. Implementing Steps. In the balanced-yielding support technology, the stress distribution of the tunnel surrounding rock can be analyzed through theoretical analysis, numerical calculation, and other methods. According to the stress distribution of the surrounding rock, the cross-sectional shape of the tunnel and the bolt-cable parameters can be determined. Then, the reasonable structure of the anchor cable is designed to pave the way for the balanced-yielding support technology. The specific implementing steps are shown in Figure 2.

According to the above implementation steps, the balanced-yielding support technology was used to control the Shangping tunnel of Huafeng Mine.

4. Stress Distribution of the Tunnel Surrounding Rock with Different Section Shapes

4.1. In Situ Stress Analysis. The in situ stress was measured by the hydraulic fracturing technique. A total of 3 monitoring points were selected. The first monitoring point was located at the -1100 level, where the buried depth of the tunnel was about 1220 m. The second monitoring point was located 65 m north of the sixth Shimen, where the buried depth of the tunnel was about 1130 m. The third monitoring point was located 45 m east of Shimen in the -920 level, where the buried depth of the tunnel was about 1040 m. The measurement results of the in situ stress are shown in Table 1.

Table 1 shows that the buried depths of the three monitoring points were all over 1000 m, especially for the deepest reaching 1220 m. The maximum horizontal principal stresses of the three monitoring points were 42.2 MPa, 36.15 MPa, and 31.35 MPa, respectively. So, the maximum horizontal principal stress was greater than 30 MPa. The direction of the maximum horizontal principal stress was mainly in N3°E~N23.5°W. The minimum horizontal principal stresses of the three monitoring points were 22.8 MPa, 19.1 MPa, and 16.2 MPa, respectively, which were all greater than 15 MPa. It showed that the vertical stress, the maximum horizontal principal stress, and the minimum horizontal principal stress gradually increased with the increase of the buried depth. The ratios of the maximum horizontal principal stress to the vertical stress at the three monitoring points were 1.305, 1.207, and 1.133, respectively, indicating that the initial rock stress field was dominated by horizontal stress. And the ratio gradually increased as the depth increases, and that was the deeper the mining depth, the more obvious the effect of tectonic stress.

4.2. Stress Distribution of the Surrounding Rock

4.2.1. Rectangle and Vertical-Wall Semicircular Arch Tunnels. According to the mining geological conditions of Huafeng Mine, the length, width, and height of the numerical model were 220 m, 150 m, and 200 m. The inclination angle of the coal-rock strata was 33°. The mechanical parameters of the 6th coal roof and floor strata are shown in

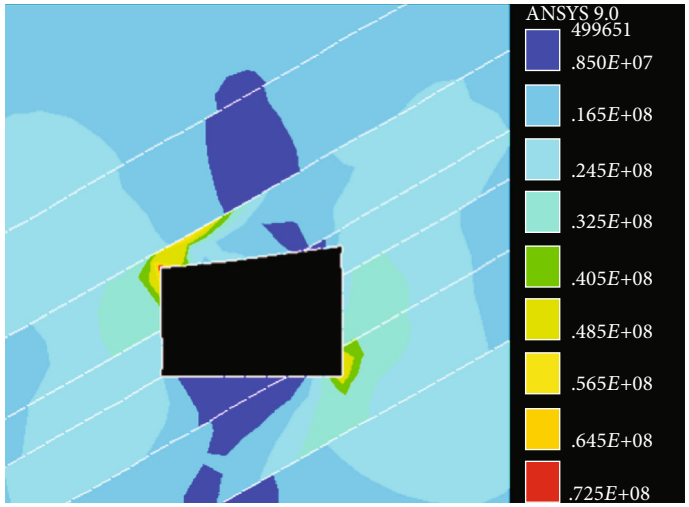

(a) Shear stress distribution

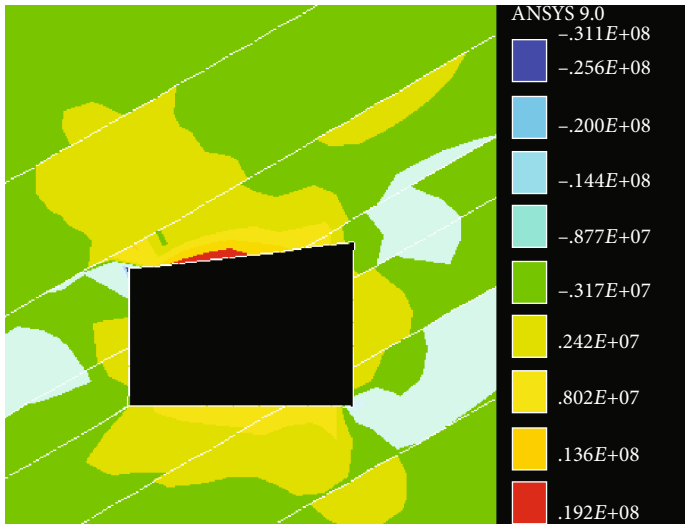

(b) Maximum principal stress distribution

Figure 6: Nephogram of the stress distribution of the trapezoidal tunnel surrounding rock.

Figure 7: The distribution of the SF of the unsupported tunnel.

Table 2. In order to simplify the force of the overlying strata, a uniform load was applied to the upper boundary of the model. The load was equal to the weight of the overlying rock. The depth was 920 m, so the stress applied on the upper boundary was 23.46 MPa. Single-directional restraints were imposed on both sides of the model, and bidirectional

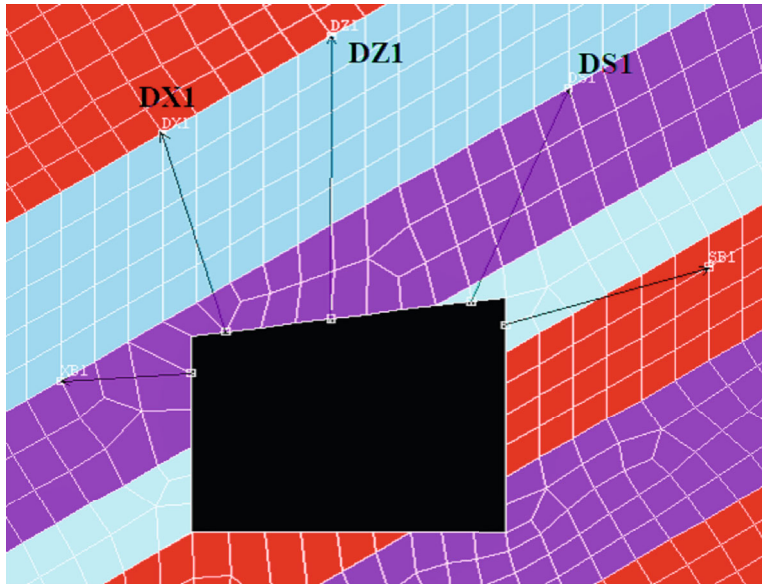

Figure 8: The stress distribution path.

constraint was imposed on its bottom boundary. The model took the Mohr-Coulomb constitutive relation. According to the implementing steps of the balanced-yielding support technology, the purpose was to select a reasonable tunnel cross-sectional shape. Firstly, the common rectangle and vertical-wall semicircular arch tunnels were selected for stress analysis.

Figures 3 and 4 show the stress distributions of the surrounding rocks of rectangular and vertical-wall semicircular arch tunnels. It could be seen from Figure 3 that the stress concentration occurred at the junction of the left side and the roof and the intersection of the right side and the floor of the rectangular tunnel. The shear failure of the tunnel roof would occur in the left half. The coal wall on the left side would be severely damaged. Figure 4 shows that the stress concentration occurred at the left half of the vertical-wall semicircular arch tunnel roof. The degree of stress concentration on the left vertical-wall was much greater than that on the right vertical-wall. The arched roof of the tunnel would cause shear failure due to extrusion. The coal wall of the left straight wall would be greatly deformed. So, in the engineering application, the support strength of the left side and floor of the tunnel should be improved, especially to ensure the support effect of the bolts in bottom corner.

4.2.2. The Mechanism of Stress Concentration. Taking the vertical-wall semicircular arch tunnel as an example, the mechanism of stress concentration was analyzed. The immediate roof of the Shangping tunnel was low-strength siltstone, which would inevitably increase the damage to the surrounding rock. In addition, under the influence of the component force of the rock layer's own weight stress in the inclined direction and the horizontal stress, the stress distribution of the surrounding rock of the tunnel was uneven, especially in the local stress concentration. However, the component force of the rock layer's own weight stress in the inclined direction had different effects on the two sides of the tunnel. This effect is shown in Figure 5. The red streamline indicated the rock layer's own weight stress curve in the inclined direction. Figure 5 shows that the stress concentration occurred at the top corner of the right side and the bottom corner of the left side of the tunnel. In addition, the stress release occurred at the top corner of the left side and the bottom corner of the right side of the tunnel.

The component force of the rock layer's own weight stress in the inclined direction was the basic reason of the rock layer's shear slip. The shear slip was the main reason for the shear stress between layers. The shear stress caused the stress concentration at the top corner of the right side and the bottom corner of the left side. So, in order to reduce the stress concentration here, the roof and floor could be changed to follow the direction of the rock layer as much as possible. This could reduce the degree of shear failure of the tunnel surrounding rock. In addition, considering the basic requirements of the tunnel for pedestrians, transportation, and pipelines, the tunnel floor must be level. So, the overall shape of the tunnel could be a trapezoid with an inclined roof.

4.2.3. Stress Distribution of Trapezoidal Tunnel. Based on the above theoretical analysis and numerical simulation, considering the combined effect of the component force of the rock layer's own weight stress in the inclined direction and the horizontal stress, the roof direction of the trapezoidal tunnel was designed roughly along the combined direction of the rock layer and the horizontal. The width and the height of the two sides of the tunnel were designed to be 3.8 m, 3.0 m, and 2.5 m, respectively. The stress distribution of the surrounding rock of trapezoidal tunnel is shown in Figure 6.

It could be seen from Figure 6, under the combined effect of the component force of the rock layer's own weight stress in the inclined direction and the horizontal stress, the

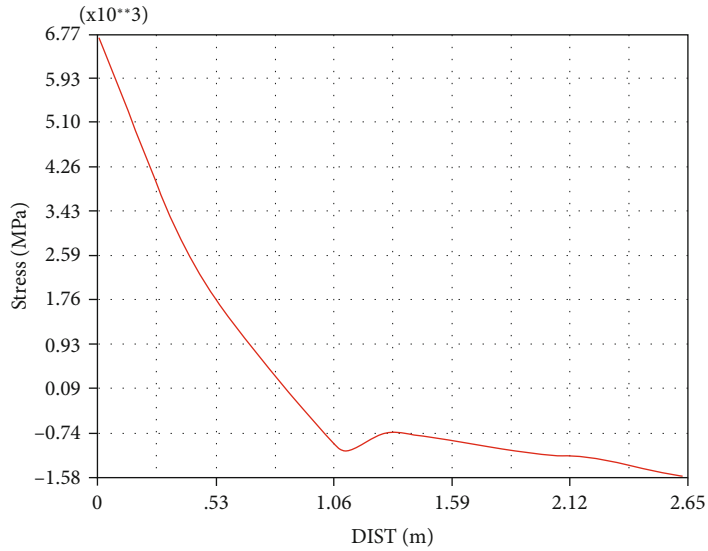

(a) Dx1

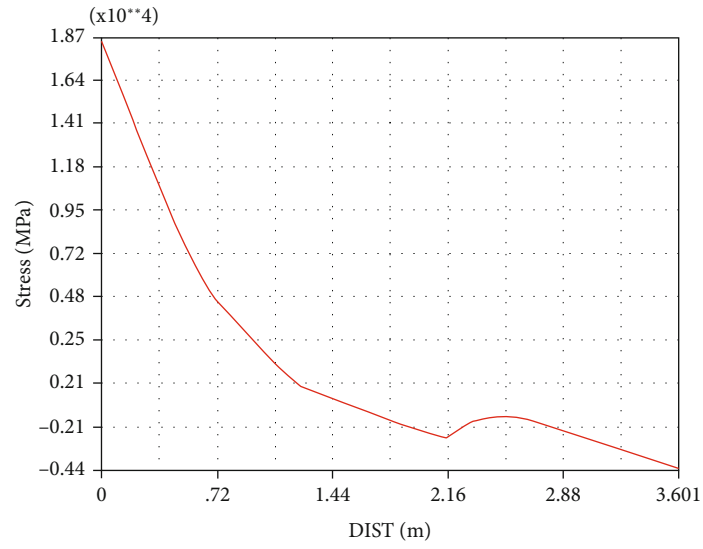

(b) Dz1

Figure 9: Continued.

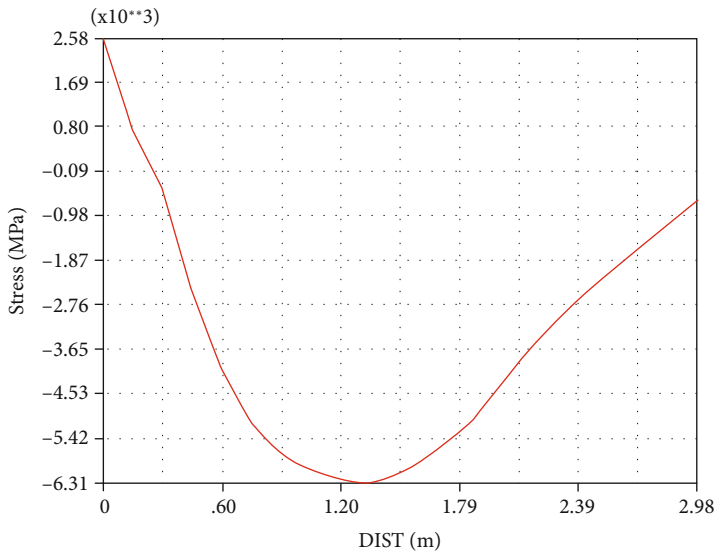

(c) Ds1

Figure 9: The maximum principal stress along each path.

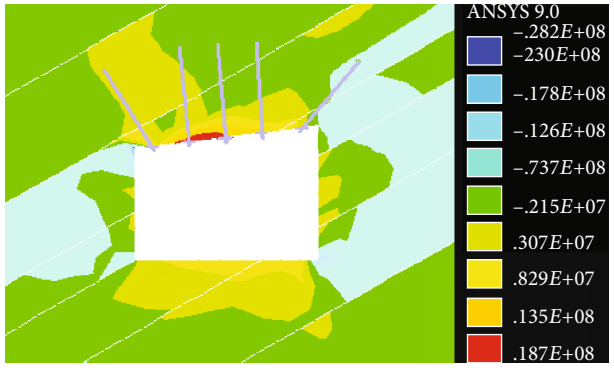

Figure 10: The stress distribution of the tunnel roof with the prestressed bolts of 20 kN.

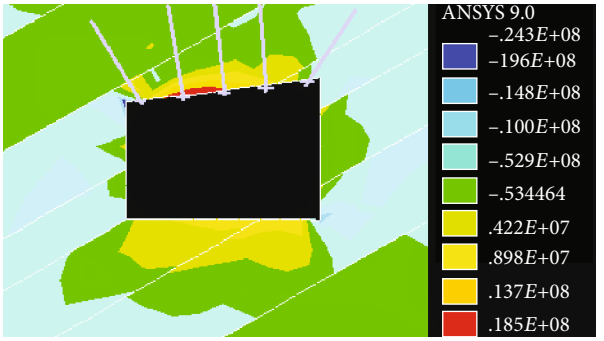

Figure 11: The stress distribution of the tunnel roof with the prestressed bolts of 40 kN.

stress concentration still occurred at the top corner of the left side and the bottom corner of the right side of the tunnel, and the stress release occurred at the other two opposite angles. The shear stress at the top corner of the left side was generally 4.5 MPa, with the maximum of 7.25 MPa. The stress concentration penetrated the surrounding rock to the rock interface. The shear stress at the bottom corner of the right side of the tunnel was 4.2 MPa, which was slightly smaller than that at the top corner of the left side. In addition, the shear stress at the two sides was about 3 MPa. It showed that the stress concentration of the surrounding rock was not large, which was consistent with the theoretical analysis results. The inclined roof of the trapezoidal tunnel effectively weakened the effect of the component force of the rock layer's own weight stress in the inclined direction. The maximum roof tensile stress and the maximum principal stress peak of the tunnel were both located on the left half of the inclined roof. In the area of maximum roof tensile stress here, the anchor cables should be arranged perpendicular to the rock layer for reinforcement. In addition, since the stress concentration was the most serious at the top corner of the left side, an inclined anchor cable was arranged to balance the stress concentration here.

5. Balanced-Yielding Support Scheme

Based on the trapezoidal tunnel, in order to make the surrounding rock deformation basically the same, a balanced-yielding support scheme was designed by increasing the support strength in the high stress concentration area. This scheme was based on the high-strength yielding bolt support system. Next, the bolt support parameters and yield structure were designed.

5.1. Bolt Length. According to Mohr-Coulomb criterion, the safety factor (SF) of rock failure can be calculated [26–29]. The area where the SF of the tunnel surrounding rock was greater than 1.5 was safe. The area with SF less than 1.5 was unstable, so the support control was needed. The distribution of the SF of the unsupported tunnel is shown in Figure 7. In order to further determine the length of bolts

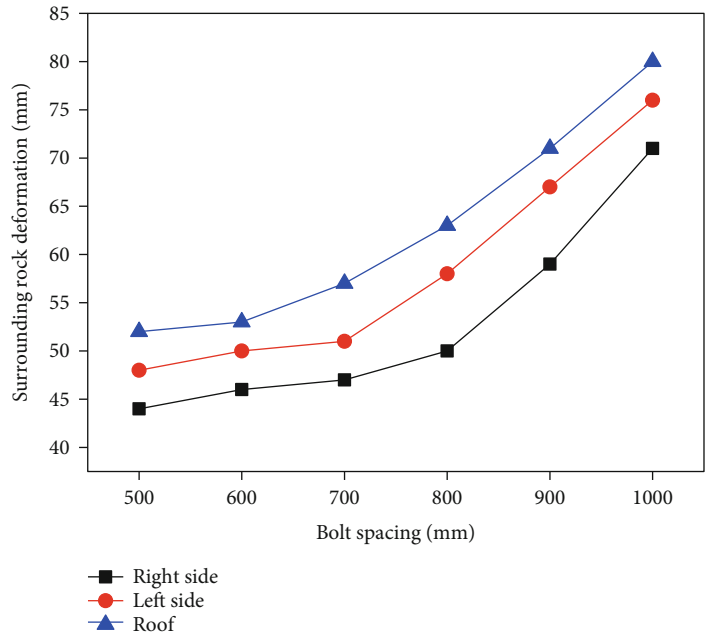

(a) The spacing distances of bolt

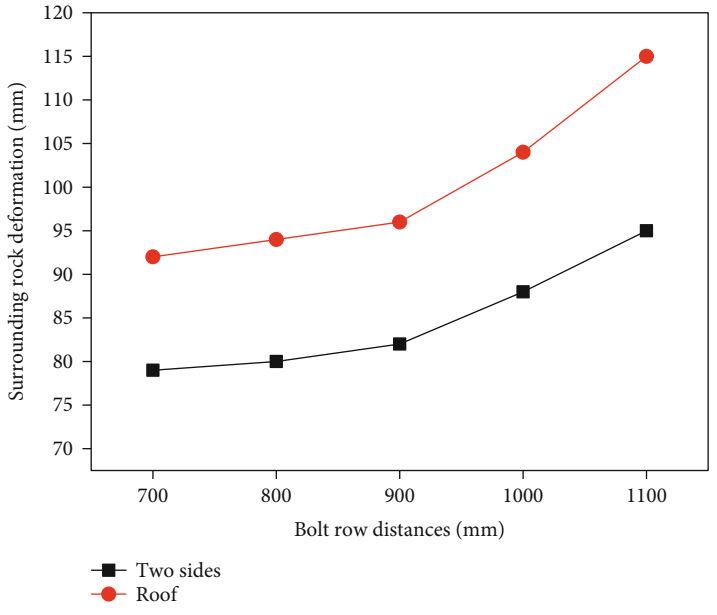

(b) The row distances of bolt

Figure 12: The relationships between the spacing and row distances of bolt and surrounding rock deformation.

at different positions, three paths, Dx1, Dz1, and Ds1, were selected to analyze the stress distribution. The stress distribution path is shown in Figure 8. The maximum principal stress along each path is shown in Figure 9.

It could be seen from Figures 8 and 9 that under the influence of tunnel excavation, the maximum height of the tensile stress zone at the top corner of the left side was about 0.8 m. The maximum height of the tensile stress zone of the roof rock layer was about 1.2 m. The maximum height of the tensile stress area at the top corner of the right side was about 0.2 m. So, the maximum height of the tensile stress zone of the roof was 1.2 m. The bolt should be anchored in the rock layer outside the tensile stress zone to effectively control its damage. So, the length of the tensile section of the bolt-rod should be greater than the maximum depth of the tensile stress zone. It was assumed that the length of the bolt outside the tensile stress zone was 0.6 m, and the exposed length of the bolt in the tunnel was 0.1 m. It was calculated that the length of the roof bolt should be 1.9 m. In addition, because the immediate roof of the tunnel was 1.8 m thick siltstone with poor stability, the bolt needed to pass through the siltstone and be anchored into the stable rock stratum. So, the length of the tunnel roof bolt was designed to be 2.5 m.

Figure 13: The yielding pipe before and after work.

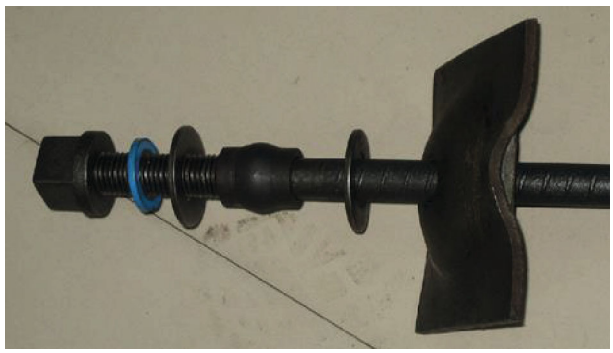

Figure 14: The high-strength prestressed yield bolt.

It could be seen from Figure 7 that the safety factor at the 1.4 m and 1.8 m depth of the two sides reached 1.3 and 1.5. The bolts at the two sides should be anchored to the area where the SF was less than 1.5, so the length of the bolts should be more than 1.8 m. Due to the large burial depth, "coal burst" frequently occurred during the tunneling process. In addition, the horizontal stress was relatively high. So, the length of the roof bolt and the side bolt was determined to be 2500 mm. Due to the large stress concentration on the left side of the tunnel, the bolt support density of the left side should be increased to balance the stress of the surrounding rock.

5.2. Prestress of Bolt. According to the optimal bolt length of 2500 mm determined in Section 5.1, the prestress of the bolt was investigated. As the roof rock layer was the most representative, this part only studied the support effect of prestressed bolts on the tunnel roof. Four bolts were arranged on the tunnel roof, and the bolts at the two corners were inclined. The prestressing force was selected as 20 kN and 40 kN, respectively. Figures 10 and 11 show the stress distributions of the tunnel roof with the prestressed bolts of 20 kN and 40 kN, respectively.

It could be seen from Figure 10 that when the prestress was 20 kN, the tensile stress area of the tunnel roof was relatively large. And the number of separations in the roof rock layer within 1000 mm was relatively large. It showed that the prestressed bolt with the prestress of 20 kN could not meet the requirements of tunnel support. So, it was necessary to increase the prestress of bolt. It could be seen from Figure 11 that when the prestress was 40 kN, the tensile stress area of the tunnel roof was basically eliminated. And the roof separation was basically closed. It showed that the prestressed bolt with the prestress of 40 kN could basically control the roof rock layer actively. In application, in order to ensure the supporting effect, the prestress of the bolt was designed to be 50 kN.

5.3. Spacing and Row Distances of Bolt. Based on the abovementioned bolt length of 2500 mm, the spacing and row distances between bolts were investigated by numerical simulation. According to the above numerical model, the deformations of tunnel with bolt spacing of 500 mm, 600 mm, 700 mm, 800 mm, 900 mm, and 1000 mm and bolt row distances of 700 mm, 800 mm, 900 mm, 1000 mm, and 1100 mm were calculated, respectively, without anchor cable. The relationships between the spacing and row distances of bolt and surrounding rock deformation are shown in Figure 12.

It could be seen from Figure 12(a) that when the bolt spacing on the right side was less than 800 mm, the change of surrounding rock deformation was no longer obvious. So, the optimal spacing distance between the right side bolts was 800 mm. When the bolt spacing on the left side was less than 700 mm, the change of surrounding rock deformation was no longer obvious. So, the optimal spacing distance between the left side bolts was 700 mm. When the roof bolt spacing was less than 700 mm, the change rate of surrounding rock deformation would gradually decrease as the spacing continues to decrease. When the roof bolt spacing was less than 600 mm, the surrounding rock deformation would basically no longer change. So, considering the cost and effect of support, the roof bolt spacing was selected as 650 mm. Figure 12(b) shows that when the bolt row distances on the roof and two sides were less than 900 mm, the changes of surrounding rock deformations were no longer obvious. So, the bolt row distances were selected as 900 mm. According to the above analysis, the spacing and row distances of the bolts on roof, right side and left side, were 650×900 mm, 800×900 mm, and 700×900 mm, respectively.

5.4. Structural Design of Prestressed Yield Bolt. Based on the abovementioned bolt supporting parameters, a yielding structure was installed on the high-strength prestressed bolt to improve its supporting effect. On the one hand, the yielding structure could protect the bolt-rod from breaking. On the other hand, the bolts in the stress concentration area were first deformed, which could relieve the excessive force of the bolt-rod, reduce the stress concentration, and maintain the overall force balance of the surrounding rock.

According to the geology and mining conditions of Huafeng Mine, high-strength yield bolts were selected. The yield strength of the bolt-rod was greater than 500 MPa. The yield load and tensile load of the high-strength bolt with the diameter of 25 mm were greater than 170 kN and 240 kN, respectively [30, 31]. According to the tensile test result of the bolt-rod in laboratory, the actual yield load of the bolt was about 220 kN. So, the start-up load of the yielding structure should be designed to be 170-200 kN. According to the characteristics of in situ stress and the surrounding rock, it was determined that the maximum yielding distance was

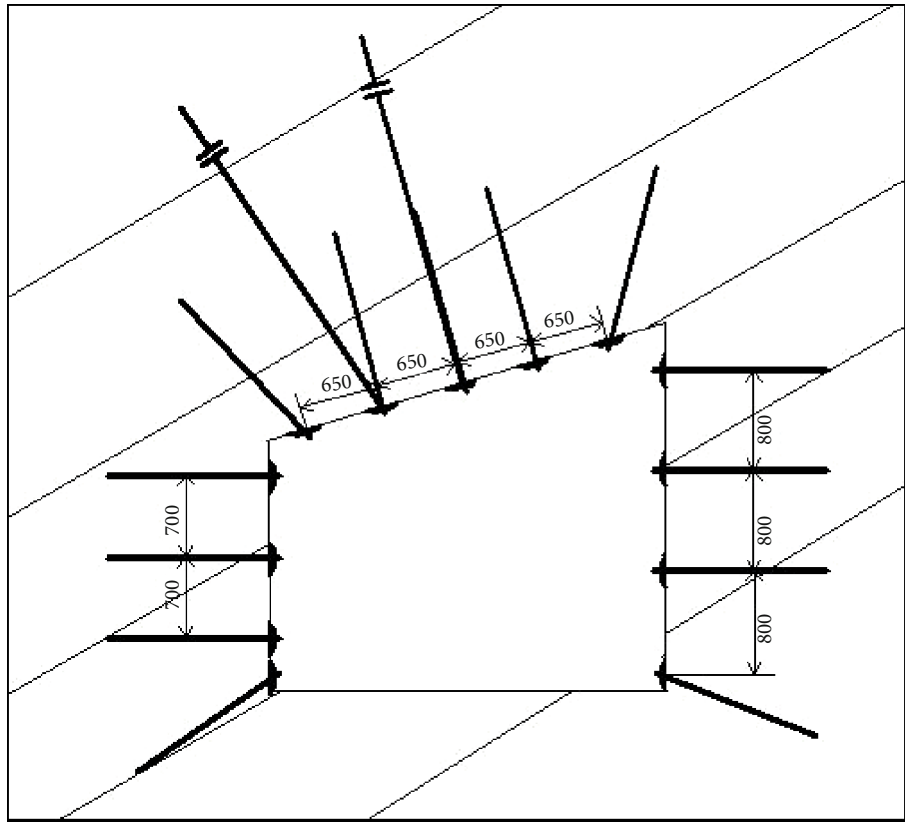

Figure 15: The schematic diagram of the tunnel support scheme.

not less than 20 mm. The stability of the yielding structure was measured by the yielding stability coefficient. It should not be greater than 2 kN/mm. The yielding stability coefficient is as follows:

$$W = \frac{R_t - R_0}{D}, \tag{1}$$

where W is the yielding stability coefficient, T/mm. R_t is the terminal load of yielding structure, kN. R_0 is the start-up load of the yielding structure, kN. D is the maximum yielding distance, mm.

Several groups of laboratory tests were carried out on the yielding pipe. The yielding pipe before and after work is shown in Figure 13. According to the scattered points of the experiment, the regression curve was obtained. The regression curve equation of the yielding pipe is as follows:

$$\begin{aligned} y &= -0.0004x^4 + 0.0305x^3 - 0.8661x^2 \\ &\quad + 10.164x - 23.624, \\ R^2 &= 0.9125, \end{aligned} \tag{2}$$

where R^2 was 0.91245, indicating that the parameters and performance of the yielding pipe were reliable. Therefore, the start-up load of the yielding pipe was 190 kN, the maximum yielding distance of the yielding pipe was 25 mm, the yielding stability coefficient was 1.6 kN/mm < 2 kN/mm. So, the yielding pipe can meet the yielding requirement.

5.5. Balanced-Yielding Support Scheme. Based on the above research results, a balanced-yielding support scheme for Shangping tunnel was proposed. The shape of the tunnel section was trapezoidal. The width and heights of the tunnel were 3.8 m, 3.0 m, and 2.5 m, respectively. The high-strength prestressed yield bolt (as shown in Figure 14) with diameter of $\Phi 25 \times 2500$ mm was selected. The spacing and row distances of the bolts on roof, right side and left side, were 650×900 mm, 800×900 mm, 700×900 mm, respectively. The prestress of the bolts was not less than 50 kN. Each bolt matched two resins of Z2850. The start-up load of the yielding pipe was 190 kN, the maximum yielding distance of the yielding pipe was 25 mm, and the yielding stability coefficient was 1.6 kN/mm. The prestress of the high-strength anchor cable with the model of $\Phi 17.8 \times 4500$ mm was 100-150 kN. Each anchor cable matched two resins of Z2350. The metal mesh of $(100 \sim 80) \times (100 \sim 80) \times (6 \sim 8)$ mm and the W steel belt of 2.75×270 mm were laid on the tunnel surface. Figure 15 is a schematic diagram of the tunnel support scheme.

6. Engineering Application and Evaluation

In order to evaluate the control effect of the balanced-yielding support scheme on the surrounding rock of the Shangping tunnel, a 100 m test tunnel was selected. There were 5 observation stations. The third observation station was selected for comparative analysis with the tunnel

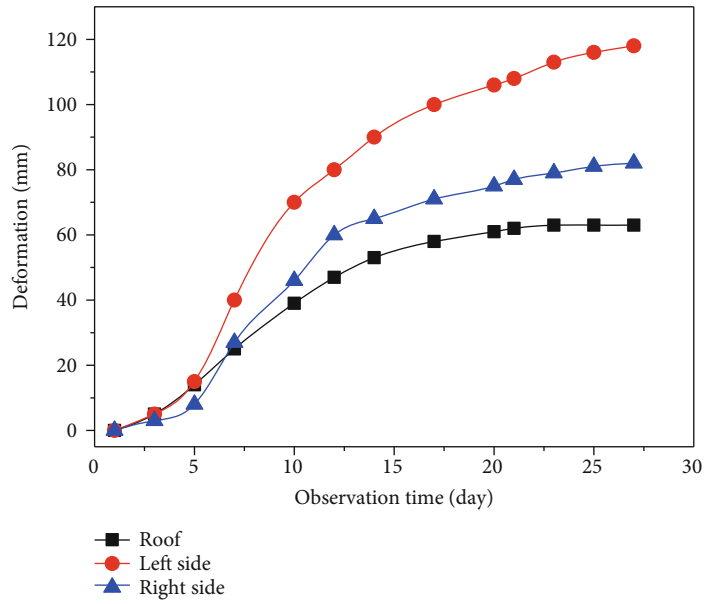

(a) Deformation

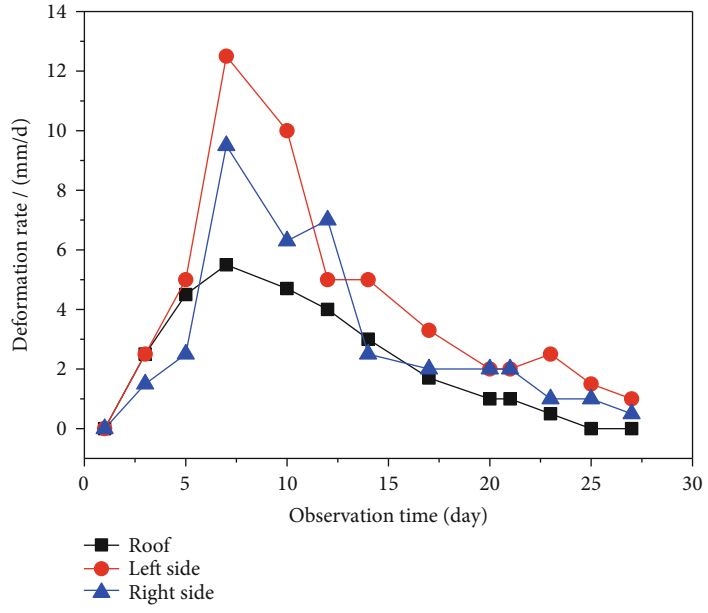

(b) Deformation rate

Figure 16: Deformation of the tunnel surrounding rock supported by the original scheme.

supported by the original scheme. It mainly included deformation and separation observation.

6.1. Deformation Observation

6.1.1. Tunnel Supported by the Original Scheme. The tunnel was a vertical-wall semicircular arch. The deformation of the tunnel surrounding rock supported by the original scheme is shown in Figure 16.

Figure 16 shows that the surrounding rock deformed severely within 14 days after excavation. During this period, the deformation rate of the tunnel surface was relatively large, which led to large deformation. The maximum deformation rates of the roof, left side and right side, were 5.5 mm/d, 12.5 mm/d, and 9.5 mm/d, respectively. After 14 days of excavation, the deformation rate was lower than 5 mm/d and gradually decreased with time. The surrounding rock gradually stabilized. The maximum deformation of the roof, left side and right side, was 63 mm, 118 mm, and 82 mm. That is, the total deformation of the two sides of the tunnel was 201 mm. It showed that the deformation of the two sides of the tunnel supported by the original scheme was too large, especially for the asymmetrical deformation of the two sides. The maximum deformation of the left side was 1.44 times that of the right side. This was consistent with the results of the previous numerical simulations. So, the system

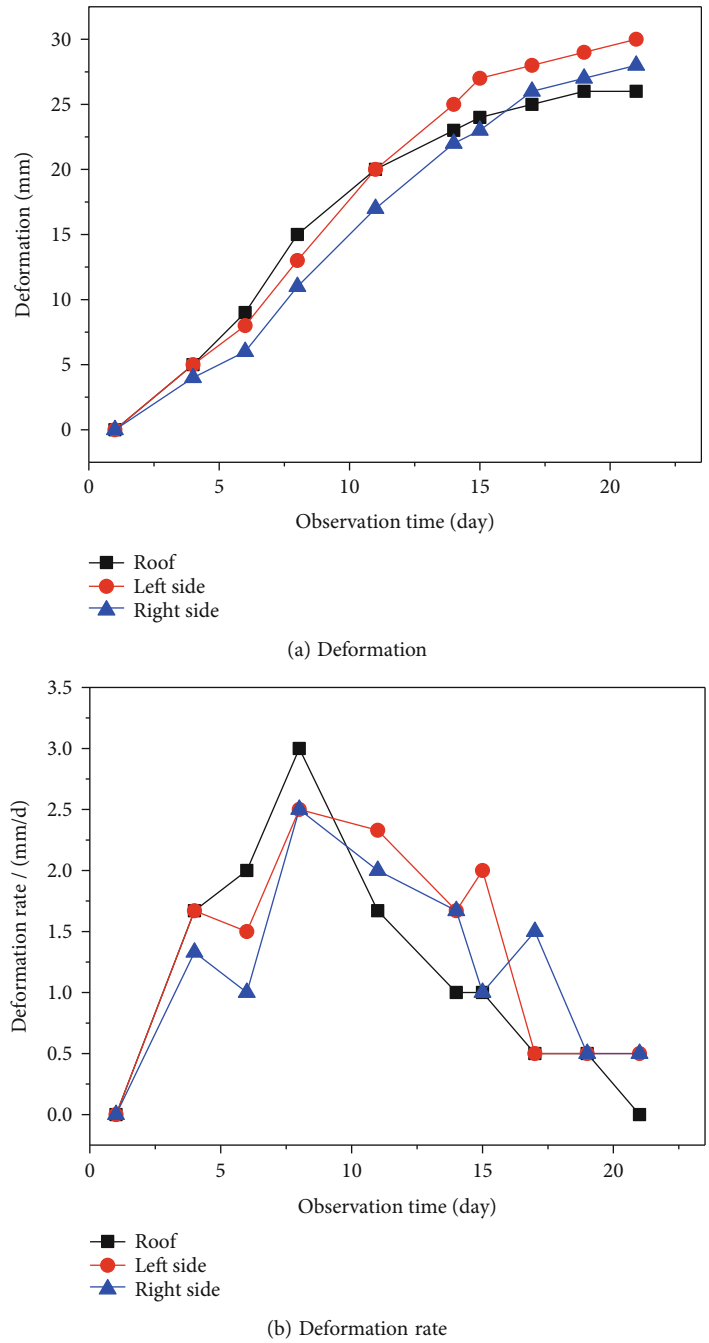

(a) Deformation

(b) Deformation rate

Figure 17: Deformation of the tunnel surrounding rock supported by the balanced-yielding support scheme.

did not fully exert its support effect. It was necessary to adjust the shape of the tunnel and optimize the support scheme.

6.1.2. Tunnel Supported by the Balanced-Yielding Support Scheme. The tunnel was trapezoidal. The deformation of the tunnel surrounding rock supported by the balanced-yielding support scheme is shown in Figure 17.

It could be seen from Figure 17 that during the excavation period, the deformation of the tunnel surrounding rock was also mainly divided into two stages. Within 15 days after excavation, the surrounding rock deformation was relatively serious. The maximum deformation rates of the roof, left side and right side, were 3 mm/d, 2.5 mm/d, and 2.5 mm/d, respectively. This was far less than the maximum deformation rate of the tunnel supported by the original scheme. After 15 days of excavation, the deformation rate was lower than 2 mm/d. The surrounding rock gradually stabilized. The maximum deformation of the roof, left side and right side, was 26 mm, 30 mm, and 28 mm. Not only the maximum deformation of the surrounding rock was much lower than that of the tunnel supported by the original scheme, but

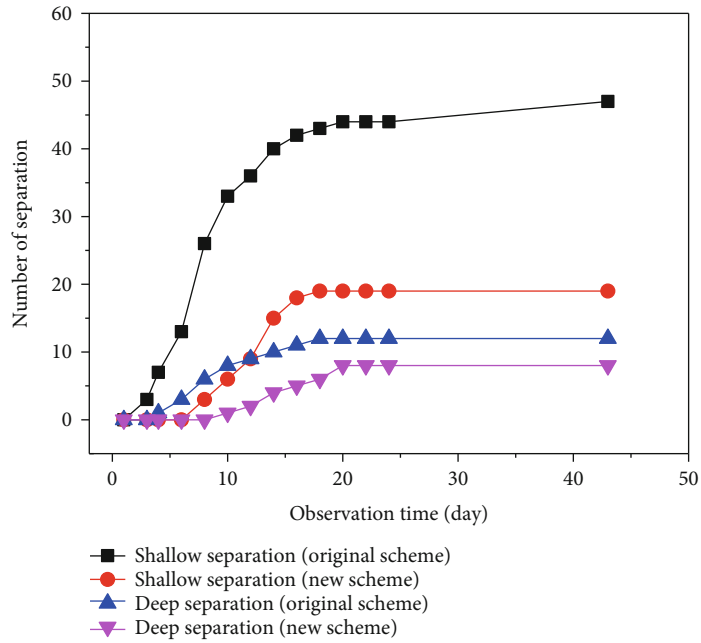

Figure 18: The roof separations of tunnels supported by the original scheme and the balanced-yielding support scheme.

also the deformations of the roof, left and right sides, were basically the same. This showed that the balanced-yielding support system had successfully realized the deformation balance of the asymmetric surrounding rock of the tunnel in the inclined rock formation, thereby controlling its overall stability.

6.2. Separation Observation. The roof separations of tunnels supported by the original scheme (vertical-wall semicircular arch tunnel) and the balanced-yielding support scheme (trapezoidal tunnel) are shown in Figure 18.

Figure 18 shows that the number of shallow separations stabilized at about 16 days. The development period of deep separation was relatively long and tended to be stable until about 20 days. The maximum amounts of the shallow and deep separations of tunnels supported by the original scheme were 47 mm and 12 mm. Its total roof separation was 59 mm. The shallow separation accounted for 79.7% of the total roof separation. This indicated that the separation was mainly concentrated in the shallow bolt support range, which further showed that the support system could not effectively control the early separation of the roof strata.

The maximum amounts of the shallow and deep separations of tunnels supported by the balanced-yielding support scheme were 19 mm and 8 mm. Its total roof separation was 27 mm. Compared with the tunnel supported by the original scheme, the amount of shallow separation was reduced by 147%. It showed that the balanced-yielding support scheme had a better effect in controlling the roof separation of the trapezoidal tunnel than the original scheme in controlling the vertical-wall semicircular arch tunnel. The performance of the support system had been better utilized. This was consistent with the monitoring results of surrounding rock deformation.

7. Conclusion

(1) An innovative balanced-yielding support technology was proposed with the engineering background. Its implementing steps mainly included in situ stress analysis, the stress distribution of the tunnel surrounding rock with different sections, the design of the support parameter for bolt-cable and yielding structure, and supporting effect evaluation

(2) The maximum horizontal principal stresses of the three monitoring points in Huafeng Mine were greater than 30 MPa. Under the influence of the component force of the rock layer's own weight stress in the inclined direction, the stress concentration occurred at the top corner of lower side and the bottom corner of the upper side of the tunnel. To reduce the stress concentration, the overall shape of the tunnel could be trapezoidal

(3) In the balanced-yielding support scheme, the high-strength prestressed yield bolt with diameter of Φ 25×2500 mm was selected. The spacing and row distances of the bolts on roof, right side and left side, were 650×900 mm, 800×900 mm, and 700×900 mm, respectively. The start-up load of the yielding pipe was 190 kN, the maximum yielding distance of the yielding pipe was 25 mm, and the yielding stability coefficient was 1.6 kN/mm

(4) In engineering application, not only the maximum deformation of the tunnel supported by the balanced-yielding support scheme was much lower than that of the tunnel supported by the original scheme, but also the deformations of the roof, left

and right sides, were basically the same. Compared with the original support system, the shallow separation of the trapezoidal tunnel supported by the balanced-yielding support system had been reduced by 147%

Data Availability

The data are available and are explained in this article; readers can access the data supporting the conclusions of this study.

Conflicts of Interest

The authors declare that there are no conflicts of interest.

Acknowledgments

This study was supported by the Key Research and Development Program of Guangxi (No. AB20238036).

References

[1] M. Zhang and Y. Zhang, "Stability evaluation method for gateways in closely spaced coal seams and surrounding rock control technology," *Arabian Journal for Science and Engineering*, vol. 20, no. 10, pp. 5469–5485, 2018.

[2] H. Wang, C. Jiang, P. Q. Zheng, N. Li, and Y. B. Zhan, "Deformation and failure mechanism of surrounding rocks in crossed-roadway and its support strategy," *Engineering Failure Analysis*, vol. 116, article 104743, 2020.

[3] Q. Wang, Q. Qin, B. Jiang, H. C. Yu, R. Pan, and S. C. Li, "Study and engineering application on the bolt-grouting reinforcement effect in underground engineering with fractured surrounding rock," *Tunnelling and Underground Space Technology*, vol. 84, pp. 237–247, 2019.

[4] Z. Zhang, F. Chen, N. Li, G. Swoboda, and N. Liu, "Influence of fault on the surrounding rock stability of a tunnel: location and thickness," *Tunneling and Underground Space Technology*, vol. 61, pp. 1–11, 2017.

[5] J. P. Zhang, L. M. Liu, Q. H. Li et al., "Development of cement-based self-stress composite grouting material for reinforcing rock mass and engineering application," *Construction and Building Materials*, vol. 201, pp. 314–327, 2019.

[6] J. Zhang, L. Liu, J. Cao, X. Yan, and F. Zhang, "Mechanism and application of concrete-filled steel tubular support in deep and high stress roadway," *Construction and Building Materials*, vol. 186, pp. 233–246, 2018.

[7] G. S. Esterhuizen and I. B. Tulu, "Analysis of alternatives for using cable bolts as primary support at two low-seam coal mines," *International Journal of Mining Science and Technology*, vol. 26, no. 1, pp. 23–30, 2016.

[8] D. J. Hutchinson and V. Falmagne, "Observational design of underground cable bolt support systems utilizing instrumentation," *Bulletin of Engineering Geology and the Environment*, vol. 58, no. 3, pp. 227–241, 2000.

[9] C. L. Wang, G. Y. Li, A. S. Gao, F. Shi, Z. J. Lu, and H. Lu, "Optimal pre-conditioning and support designs of floor heave in deep tunnels," *Geomechanics and Engineering*, vol. 14, no. 5, pp. 429–437, 2018.

[10] Q. Wang, Z. H. Jiang, B. Jiang, H. K. Gao, Y. B. Huang, and P. Zhang, "Research on an automatic roadway formation method in deep mining areas by roof cutting with high-strength bolt-grouting," *International Journal of Rock Mechanics and Mining Sciences*, vol. 128, p. 104264, 2020.

[11] R. Peng, X. Meng, G. Zhao, Z. Ouyang, and Y. Li, "Multi-echelon support method to limit asymmetry instability in different lithology roadways under high ground stress," *Tunnelling and Underground Space Technology*, vol. 108, article 103681, 2020.

[12] J. Zhang, M. Wang, and C. Xi, "Tunnel collapse mechanism and its control strategy in fault fracture zone," *Shock and Vibration*, vol. 2021, Article ID 9988676, 10 pages, 2021.

[13] Y. R. Yang, X. Lai, P. Shan, and F. Cui, "Comprehensive analysis of dynamic instability characteristics of steeply inclined coal-rock mass," *Arabian Journal of Geosciences*, vol. 13, no. 6, 2020.

[14] P. Xiao, D. Y. Li, G. Y. Zhao, Q. Q. Zhu, H. X. Liu, and C. S. Zhang, "Mechanical properties and failure behavior of rock with different flaw inclinations under coupled static and dynamic loads," *Journal of Central South University*, vol. 27, no. 10, pp. 2945–2958, 2020.

[15] Y. Q. Cai, B. Xu, Z. G. Cao, X. Y. Geng, and Z. H. Yuan, "Solution of the ultimate bearing capacity at the tip of a pile in inclined rocks based on the Hoek-Brown criterion," *International Journal of Rock Mechanics and Mining Sciences*, vol. 125, article 104140, 2020.

[16] S. Q. He, D. Z. Song, X. Q. He et al., "Coupled mechanism of compression and prying-induced rock burst in steeply inclined coal seams and principles for its prevention," *Tunnelling and Underground Space Technology*, vol. 98, article 103327, 2020.

[17] M. C. He, Y. Y. Peng, S. Y. Zhao, H. Y. Shi, N. Wang, and W. L. Gong, "Fracture mechanism of inversed trapezoidal shaped tunnel excavated in 45° inclined rock strata," *International Journal of Mining Science and Technology*, vol. 25, no. 4, pp. 531–535, 2015.

[18] Y. C. Li, Z. Q. Zeng, and Y. C. Dong, "Limit analysis of progressive asymmetrical collapse failure of tunnels in inclined rock stratum," *Symmetry*, vol. 11, no. 7, p. 904, 2019.

[19] Z. G. Tao, C. Zhu, X. H. Zheng et al., "Failure mechanisms of soft rock roadways in steeply inclined layered rock formations," *Geomatics Natural Hazards & Risk*, vol. 9, no. 1, pp. 1186–1206, 2018.

[20] Y. C. Li and Z. Q. Zeng, "Upper bound limit analysis of unsymmetrical progressive collapse of shallow tunnels in inclined rock stratum," *Computers and Geotechnics*, vol. 116, p. 103199, 2019.

[21] Z. Z. Liang, W. C. Song, and W. T. Liu, "Theoretical models for simulating the failure range and stability of inclined floor strata induced by mining and hydraulic pressure," *International Journal of Rock Mechanics & Mining Sciences*, vol. 132, article 104382, 2020.

[22] X. Y. Sun, C. H. Ho, C. Li, Y. Xia, and Q. Zhang, "Inclination effect of coal mine strata on the stability of loess land slope under the condition of underground mining," *Natural Hazards*, vol. 104, no. 1, pp. 833–852, 2020.

[23] M. Wang, G. L. Guo, X. Y. Wang, Y. Guo, and V. Dao, "Floor heave characteristics and control technology of the roadway driven in deep inclined-strata," *International Journal of Mining Science and Technology*, vol. 25, no. 2, pp. 267–273, 2015.

[24] Q. Ye, W. J. Wang, G. Wang, and Z. Z. Jia, "Numerical simulation on tendency mining fracture evolution characteristics of

overlying strata and coal seams above working face with large inclination angle and mining depth," *Arabian Journal of Geosciences*, vol. 10, no. 4, 2017.

[25] X. M. Sun, F. Chen, M. C. He, W. L. Gong, H. C. Xu, and H. Lu, "Physical modeling of floor heave for the deep-buried roadway excavated in ten degree inclined strata using infrared thermal imaging technology," *Tunnelling and Underground Space Technology*, vol. 63, pp. 228–243, 2017.

[26] F. Hadi, "Risk assessment and prediction of safety factor for circular failure slope using rock engineering systems," *Environmental Earth Sciences*, vol. 76, no. 5, pp. 1–9, 2017.

[27] M. Sari, "Evaluation of rock slopes susceptible to circular failures using logistic and multiple regression models," *Arabian Journal of Geosciences*, vol. 13, no. 2, 2020.

[28] M. A. Sánchez, F. Alberto, T. Carmen, and I. Eneko, "Geological risk assessment of the area surrounding Altamira Cave: a proposed Natural Risk Index and Safety Factor for protection of prehistoric caves," *Engineering Geology*, vol. 94, no. 3-4, pp. 180–200, 2007.

[29] K. Emad, A. Mehdi, H. M. Farouq, and M. Edmund, "Statistical analysis of bimslope stability using physical and numerical models," *Engineering Geology*, vol. 254, pp. 13–24, 2019.

[30] Y. Yasuhiro, Z. Y. Zhao, W. Nie, D. Kensuke, I. Keita, and O. Yuko, "Experimental and numerical study on the interface behaviour between the rock bolt and bond material," *Rock Mechanics and Rock Engineering*, vol. 52, no. 3, pp. 869–879, 2019.

[31] Y. Yasuhiro, Z. Y. Zhao, W. Nie et al., "Development of a new deformation-controlled rock bolt: numerical modelling and laboratory verification," *Tunnelling and Underground Space Technology*, vol. 98, article 103305, 2020.